• "This is the peer reviewed version of the following article: [Smith TD, VB DeLeon, TP Eiting, HM Corbin, KP Bhatnagar, SE Santana. 2022. Venous networks in the upper airways of bats: A histological and diceCT study. Anatomical Record, 305: 1871-1891. DOI: 10.1002/ar.24762], which has been published in final form at [Link to final article using the DOI]. This article may be used for non-commercial purposes in accordance with Wiley Terms and Conditions for Use of Self-Archived Versions."

# Venous networks in the upper airways of bats: A histological and diceCT study

Timothy D. Smith,<sup>1</sup> Valerie B. DeLeon,<sup>2</sup> Thomas P. Eiting,<sup>3</sup> Hayley M. Corbin,<sup>1</sup> Kunwar P. Bhatnagar,<sup>4</sup> Sharlene E. Santana<sup>5</sup>

1, School of Physical Therapy, Slippery Rock University, Slippery Rock, PA 16057; 2, Department of Anthropology, University of Florida; 3, Department of Neurobiology and Anatomy, Brain Institute, University of Utah; 4, Department of Anatomical Sciences and Neurobiology, University of Louisville, Louisville, KY; 5, Department of Biology and Burke Museum of Natural History and Culture, University of Washington, Seattle, WA

Funding: NSF; grant numbers BCS-1830894, BCS-1830919, IOS-1557125

Correspondence to:

Address: Tim D. Smith, Ph.D.

School of Physical Therapy

Slippery Rock University

Slippery Rock, PA 16057

E-mail: timothy.smith@sru.edu

#### **Abstract**

Our knowledge of nasal cavity anatomy has grown considerably with the advent of microcomputed tomography (CT). More recently, a technique called diffusible Iodine-based Contrastenhanced CT (diceCT) has rendered it possible to study nasal soft tissues. Using diceCT and histology, we aim to (1) explore the utility of these techniques for inferring the presence of venous sinuses that typify respiratory mucosa, and (2) inquire whether distribution of vascular mucosa may relate to specialization for derived functions of the nasal cavity (i.e., nasal-emission of echolocation sounds) in bats. Matching histology and diceCT data indicate that diceCT can detect venous sinuses as either darkened, "empty" spaces, or radio-opaque islands when blood cells are present. Thus, we show that diceCT provides reliable information on vascular distribution in the mucosa of the nasal airways. Among the bats studied, a non-echolocating pteropodid (Cynopterus sphinx) and an oral-emitter of echolocation sounds (Eptesicus fuscus) possess venous sinus networks that drain into the sphenopalatine vein rostral to the nasopharynx. In contrast, nasopharyngeal passageways of nasal-emitting hipposiderids are notably packed with venous sinuses. The mucosae of the nasopharyngeal passageways are far less vascular in nasalemitting phyllostomids, in which vascular mucosae are more widely distributed in the nasal cavity, and in some nectar-feeding species a particularly large venous sinus is adjacent to the vomeronasal organ. Therefore, we do not find a common pattern of venous sinus distribution associated with nasal emission of sounds in phyllostomids and hipposiderids. Instead, vascular mucosa is more likely critical for air-conditioning and sometimes vomeronasal function in all bats.

Key words: Chiroptera, mucosa, epithelium, vascular

### 1 INTRODUCTION

The mammalian nasal cavity bears dual function as the home of a sensory organ for chemosensation (olfaction), and as a conduit for air during respiration (Negus, 1958; Hillenius, 1992). To accomplish respiratory function, a large amount of nasal surface area is lined with vascular glandular mucosa composed of epithelium plus underlying connective tissue, or lamina propria. This "respiratory mucosa" keeps inspired air moistened and warmed, and traps dust, which the motile epithelial cilia propel toward the pharynx (Harkema, 2006). The respiratory mucosa is thus a critical air-conditioning system that protects the lower airways.

Numerous studies have mapped the distribution of different epithelium types within the nasal airways, establishing that scroll-shaped or folded evaginations of bone – called turbinals – increase surface area for olfactory or respiratory mucosa in a broad array of mammals (e.g., Adams, 1972; Bhatnagar and Kallen, 1975; Gross et al., 1982; Smith et al., 2012; Martinez et al., 2020). Turbinals may be specialized for respiration or olfaction, or possess dual specialization for these functions (Smith et al., 2007, 2011, 2019; Yee et al., 2016). Whereas we continue to amass a better comparative understanding of the nasal cavity, other more caudal parts of the respiratory tract are relatively understudied. In particular, the pharynx is an adjoining space with multiple functions (e.g., respiration, swallowing) that remains largely unexplored (Smith, 1992; Pagano, 2014). Therefore, qualitative and quantitative descriptions of the anatomy of these airways are still needed for a better understanding of their function and adaptive evolution across species. In the present study, we provide a detailed, comparative examination of the entire nasal and pharyngeal airways in selected bat species.

### 1.1 Comparative anatomy of the nasal and nasopharyngeal passageways in mammals

The mammalian nasal cavity is divided into right and left nasal passages (or fossae) by a midline nasal septum (Harkema, 2006). In humans, apes and many monkeys, the nasal fossae end ventrally at choanal apertures, which are paired portals that allow inspired air to flow from the nasal cavity into the pharynx (Smith et al., 2015). In most other mammals, the main nasal chamber becomes divided in two by a horizontal plate of bone (the transverse lamina) which divides a compartment specialized for olfaction dorsal to it, from a respiratory conduit ventral to it. The respiratory conduit is termed the nasopharyngeal duct and may be divided into two sides by the vomer for part of its length. This duct ends with the soft palate, where the duct(s) joins the pharynx. Although this duct(s) is developmentally part of the nasal cavity (Smith and Rossie, 2008), here we discuss the duct and the remainder of the nasal cavity as *functionally* distinct regions, based on airflow patterns (Eiting et al., 2015, and see below).

Within each chamber, a vestibule is found most anteriorly, bearing stratified squamous epithelium. Beyond the vestibule is the main nasal chamber, lined primarily by two epithelial types, respiratory and olfactory (we exclude from discussion a third type, "transitional epithelium," which is lesser in surface area, and of less understood function; Harkema, 2006).

The majority of mammals have greater complexity of the nasal fossae than humans by virtue of more complex and prolonged development of turbinals (see below), and accessory compartments called recesses (Ito et al., 2021; Smith et al., 2021). Most mammals have at least three more turbinal outgrowths from the ethmoid bone compared to anthropoid primates (Lundeen and Kirk, 2019), and recesses can be large, for example the paranasal recesses found in mammals with laterally positioned eyes (which provide little encroachment on the nasal region; Smith and Rossie, 2008). This complexity greatly enhanced surface area for both respiratory and olfactory mucosa (Smith et al., 2007; Yee et al., 2016). Whereas humans have a simplified nasal cavity, they have a highly complex pharynx, the shared conduit to the lower respiratory tract (via the larynx) and the alimentary tract (via the esophagus). This complexity may be attributed to the "descent" of the larynx, an ontogenetic phenomenon by which the pharynx is lengthened by differential growth during infancy, a process that also lengthens the overall vocal tract (Laitman and Reidenberg, 1993; Pagano, 2014). The epithelial lining of the nasopharyngeal and pharyngeal regions (i.e., pharynx and nasopharyngeal ducts, in species that have them) is reviewed further below.

The ventral part of the nasal cavity and nasopharyngeal ducts conduct high velocity airstreams to the pharynx (Craven et al., 2010; Eiting et al., 2015; Smith et al., 2019). Essentially, nasopharyngeal ducts prolong what is a very abrupt transition from nasal chamber to nasopharynx in humans. In the case of an undescended larynx, the more typical mammal lacks a distinct oropharynx, and thus terminology for human anatomy (naso-,oro-, laryngopharynx) is difficult to apply (see Laitman and Reidenberg, 1993; Pagano, 2014). However, the most proximal part may be homologized with the human nasopharynx by virtue of the communication of the auditory tube (Pagano, 2014).

# 1.2 Distribution of mucosae along nasal and nasopharyngeal passageways in mammals

Most mammals possess six turbinals (or turbinates, conchae), each named for bones with which they articulate in the adult skull: maxilloturbinal, nasoturbinal, and four ethmoturbinals that project far enough medially to become adjacent to the midline nasal septum (Maier, 1993; Smith et al., 2015). Here it is useful to return to consideration of the entire mucosa (epithelium plus the supporting lamina propria) for a functional consideration. Turbinals that do not reach the midline are termed frontoturbinals (those that occupy the frontal recess) or interturbinals (those tucked between more projecting turbinals). Turbinals increase the mucosal surface area by virtue of their folding or scrolling shape (Dieulafe, 1906; Negus, 1958; Harkema, 2006). Studies of a diverse array of mammals have demonstrated the dorsocaudal nasal fossa, particularly the enclosed dorsal space (the olfactory recess), are predominantly covered by olfactory mucosa (Adams, 1972; Gross et al., 1982; Smith et al., 2011, 2012; Yee et al., 2016). Most ethmoturbinals, and frontoturbinals are predominantly lined with olfactory mucosa (Adams, 1972; Gross et al., 1982; Jurcisek et al., 2003; Smith et al., 2011; Yee et al., 2016). In all

mammals, the maxilloturbinals are lined with non-olfactory mucosa, mostly respiratory type. Ventral paranasal (i.e., maxillary) recesses are non-olfactory as well, while the more dorsal frontal recess bears much olfactory mucosa (Smith et al., 2011; Yee et al., 2016).

The nasopharyngeal ducts, more rarely described, bear non-olfactory mucosa only (Smith et al., 2011). However, to our knowledge, there has been little effort to understand these passages in great detail. Recently, Curtis et al. (2020) noted nasopharyngeal ducts of Old World leafnosed bats (Hipposideridae) are lined by respiratory mucosa; the ducts of *Hipposideros* in particular are highly vascular, including venous sinuses that may warm inspired air or perhaps modulate airflow during sound transmission, as these bats emit echolocation calls through the nostrils.

The pharynx has been better studied across mammals, but with some conflicting descriptions. Pagano (2014) thoroughly reviewed descriptions in the literature, most of which centered on the human pharynx. This study confirmed that respiratory epithelium, as well as mucosal vessels consistent with air conditioning function, are present in the nasopharynx of nonhuman primates. In general, there is broad agreement that three types of epithelium (respiratory, transitional, and stratified squamous) are present in the pharynx of mammals (e.g., Leela and Kanagasuntheram,1973; Leela et al.,1974; Nakano et al., 1986). Yet, there is a need for thorough studies of the nasal and pharyngeal airways to determine to what extent mucosa specialized for air conditioning is distributed throughout the upper airways.

# 1.3 Rationale and Hypotheses:

Historically, an understanding of nasal mucosae lining has been challenging due to the need for microanatomical knowledge of tissue structure, which in turn requires time-intensive serial sectioning of heads (e.g., Adams, 1972; Bhatnagar and Kallen, 1975; Gross et al., 1982; Smith and Rossie, 2008; Yee et al., 2016). In recent years, an alternative to histology has emerged via innovative computed tomographic methodology. For example, diffusible iodine-based contrast-enhanced Computed Tomography (diceCT) has been widely used to study soft tissue structures such as muscles (e.g., Cox and Jeffery, 2011; Gignac et al., 2016; Orsbon et al., 2018; Santana, 2018; Dickenson et al., 2019) and neural structures (Vickerton et al., 2013; Hedrick et al., 2018). At present, diceCT cannot match the resolution available via histology though magnification, so identification of mucosae based on epithelial organization is crude at best. However, Yohe et al. (2019) noted that characteristics of the lamina propria are visible, such as glandular masses. As such, diceCT data has potential to help infer mucosa type.

In the present study, we employ histology and diceCT to describe the vasculature of mucosae along the nasal and nasopharyngeal airways. Our objectives are two-fold. First, by using histology and diceCT, sometimes on the same specimens, we aim to explore the utility of these techniques for inferring the presence of venous sinuses that typify respiratory mucosa. Second, since the sample studied here includes New and Old World leaf-nosed bats, all of which echolocate by means of nasal sound transmission, we investigate functional aspects of

respiratory mucosa distribution in bats. Specifically, we test the hypothesis that highly vascularized respiratory mucosae of nasopharyngeal passageways (here, meaning both the nasopharyngeal ducts and pharynx) are restricted to leaf-nosed bats, suggesting the trait is specifically related to nasophonation (Curtis et al., 2020). Alternatively, the nasopharyngeal passageways of all chiropterans may possess mucosal traits that provide air-conditioning capacity, as has recently been demonstrated in primates (Pagano, 2014).

#### 2 METHODS

### 2.1 Sample

Fifteen species were studied (20 specimens total; 19 adults, one fetus), including 13 nasal echolocating bats (10 phyllostomids and three hipposiderids), one oral echolocator (*Eptesicus fuscus*), and one non-echolocator (*Cynopterus sphinx*) (Table 1; Fig. 1). For brevity, bats will be referred to at the generic level except where multiple species were examined.

## 2.2 Imaging methods

Heads were microCT scanned at three sites, using similar parameters. *Desmodus* was scanned as Northeast Ohio Medical University (NEOMED) using the Scanco vivaCT microCT scanner (scan parameters: 70 kVp and 114  $\mu$ A; the volume was reconstructed using 20.5  $\mu$ m cubic voxels (DeLeon and Smith, 2014). Conventional  $\mu$ -CT scans of the adult *Cynopterus* and *Anoura* specimens were collected at the University of Florida with a GE V|tome|xm 240 CT scanner (scan parameters: 100 kVp; 100 mA) and reconstructed with 0.0213 x 0.0213 x 0.0213 mm cubic voxels. All other heads were scanned at University of Washington using a Skyscan 1174 or 1172  $\mu$ CT-scanner (Bruker MicroCT, Belgium) at 50 kV and 800 mA; volumes were reconstructed using 14–30  $\mu$ m voxel size (Santana, 2018).

DiceCT was also accomplished at two sites. All specimens were submerged in 20% sucrose solution for 24-48 hours prior to immersion in the staining solution. At University of Florida, the fetal and adult *Desmodus* were submerged together in 1% Lugol's solution for seven days. The adult *Anoura* and *Cynopterus* were stained in 5% Lugol's solution for seven days. At University of Washington, bat heads were submerged in a 1% w/v aqueous Lugol's iodine solution for 8-35 days. Heads were then scanned (Skyscan microCT scanners described above) at 50 kV to verify uptake and then rescanned every 3–5 days after further staining, to verify optimal uptake. The purpose of some of these scans was to demonstrate cranial muscles for a previous study (Santana, 2018), but airways are also well emphasized in most scans. Some of the scans used in the present study are stored on a related MorphoSource project page, visible publicly at: https://www.morphosource.org/projects/000365326?locale=en.

After scanning, several heads (fetal *Desmodus*, adult *Cynopterus* and *Anoura*) were prepared for paraffin histology. Hemisected heads were decalcified in a formic acid–sodium citrate solution and then returned to 10 % buffered formalin for approximately 12 h. The specimens were then processed for paraffin embedding (decalcification and embedding described in more detail by DeLeon and Smith (2014). The two paraffin blocks were sectioned at 10  $\mu$ m

thickness using a rotary microtome, and every fourth to fifth section was mounted on glass slides. Sections were stained alternately stained with Gomori trichrome and hematoxylin–eosin procedures. All other species examined by microscopy had been previously sectioned (e.g., Cooper and Bhatnagar, 1976). Sections were photographed using a MRc 150 Firewire camera attached to a Zeiss stereomicroscope (X0.64 to X1.6 magnification) and an Axiocam MRc 5 Firewire camera attached to a Leica DMLB photomicroscope (X25 to X630).

#### 2.3 Three-dimensional reconstruction

Alignment of CT and histological image datasets were accomplished using Amira postprocessing software (v. 2019.1, ThermoFisher Scientific). The plane of section of histological sections served as the "target" plane for transformation and reslicing of the µCT and diceCT volumes. Full details of the approach are provided by DeLeon and Smith (2014). Briefly, histological images were each reviewed to identify discrete, localized features that could be observed in CT images. Macro- and micro-anatomical contours of dense tissue (e.g., patterns of trabeculae and sutural intersections) were the primary resource for identifying corresponding structures in CT and histological images. At least three identifiable features on each representative histological image were required to define the plane of section. In Amira, 2D sections of the CT volume were reviewed to localize the corresponding features. Sets of three features corresponding to a given histological section were used to define oblique 2D sections through the CT volume. These oblique sections approximated the plane of section for histology. In order to virtually "re-slice" the CT volume to correspond to the histology, the 3D CT volume was transformed (i.e., rotated) into a new space defined orthogonally by the average oblique plane determined above. The volume was further resampled using Lanczos interpolation to contain cubic voxels that were a whole fraction of the spacing between contiguous histological sections. In effect, we "resliced" the original CT volume, so that a single 2D orthogonal slice of the CT volume corresponded to a single histological section (Figure 2).

### 2.3.1. Three-dimensional reconstructions of airways and venous networks

Amira software (version 2019.1) was also used to reconstruct the nasal and nasopharyngeal passageways in *Cynopterus, Triaenops* and three phyllostomid species (*Anoura, Desmodus*, and *Leptonycteris*) using diceCT scans. Partial reconstructions were also possible using diceCT scans of *Eptesicus fuscus, Hipposideros caffer* and *Uroderma bilobatum*.

Prior to reconstructions, each diceCT volume was three-dimensionally reconstructed and examined to ensure the individual CT slice levels were in the coronal plane and approximately perpendicular to the hard palate. With the exception of the scans aligned to histology, other scans were re-oriented to a coronal plane prior to segmentation; these scans were virtually "resliced" using Amira to achieve the orientation noted above. Next, the entire series of CT slices was inspected to determine if the entirety of the nasal and nasopharyngeal passageways was discernable. In many specimens, the outer boundary of the posterior region of the nasal cavity or nasopharyngeal passageways was poorly differentiated from surrounding soft tissues, limiting our ability to accurately reconstruct the airways for quantification. In most species, it was at least

possible to determine rostrocaudal end points of the nasal fossa, the paired nasopharyngeal ducts, and the common nasopharyngeal duct/nasopharynx. Dorsally, the nasal fossa ended in a blind *cul-de*-sac, the olfactory recess (Figs. 3b, d). Ventral to the olfactory recess of each side is the nasopharyngeal duct; they are separated by the transverse lamina (Figs. 3d, f). In this study, nasopharyngeal ducts were defined as the passageway ventral to the olfactory recess and also bounded inferiorly by the hard and soft palate. We also define the portion of the nasopharyngeal duct that is paired by virtue of a septum dividing the passageway into right and left sides; the septum is first formed by the vomer, and more caudally by mucosa alone. Our rationale for reconstructing this segment is based on studies demonstrating that the nasopharyngeal ducts conduct airflow rapidly (Eiting et al., 2015; Smith et al., 2019). Caudal to the paired ducts, the nasopharyngeal duct lacks a septum. This segment, here termed the "common nasopharyngeal duct" was segmented in common with the pharynx, to contrast mucosa of paired and common ducts; the latter was segmented caudally until its communication with the glottal opening into the larynx; in all cases, the pharynx was exceedingly short compared to the common nasopharyngeal duct.

In four adult bats (*Cynopterus, Anoura, Desmodus*, and *Triaenops*), the boundaries of the airways were considered adequate for volumetric reconstructions of the three segments. In *Leptonycteris*, boundaries of the airways were nearly distinct, considered suitable for heuristic images, but not quantification. In these five adult bats, plus the fetal *Desmodus*, the nasal/nasopharyngeal airways were segmented and reconstructed via automated (e.g., magic wand tool) or manually tracing methods in Amira. Typically, the airway was captured with the magic wand in every third to fourth slice and then the distance between slices was interpolated and added to the segmented volume.

Finally, venous sinus networks within nasal mucosae were segmented and reconstructed in superimposition to the airways. Prior to reconstruction, the aligned histology sections and microCT slices of fetal *Desmodus* and adult *Cynopterus* proved valuable in identifying venous sinuses. In many diceCT slices, based on a comparison to matching histology sections, the blood pooled within venous sinuses was highly radio-opaque (Figs. 2a, b). Alternatively, large venous sinuses devoid of blood cells appeared as dark spaces (e.g., Fig. 3). Thus, venous sinuses could be segmented using a high or low threshold ranges in Amira. Histology indicates that the amount of blood cells within blood vessels varied throughout the sectional series. This likely explains why sinuses may intermittently "disappear" when a single vessel is examined across diceCT slices series. To deal with this fluctuating appearance, individual venous sinuses were interpolated as necessary across slice levels in which they were determined to be indistinct, as long as the sinus followed a predictable trajectory.

### 3 RESULTS

3.1 General organization of the airways

# Cynopterus sphinx (Pteropodidae)

The facial skeleton of the adult *Cynopterus* houses a nasal cavity that is long and also expanded dorsally into a fan-shaped olfactory recess; beneath the olfactory recess, the paired portion of the nasopharyngeal ducts are elongated beyond the olfactory recess (Figs. 3a, b). The olfactory recess overlaps portions of every ethmoturbinal; only ethmoturbinal I projects rostral to the transverse lamina.

The venous sinuses of the nasal cavity drain caudoventrally along the septum and lateral wall (Fig 3). Large venous sinuses also nest within the mucosa over the "roof" of the nasal fossae rostral to the olfactory recess (Fig. 3b). All venous drainage converges to the sphenopalatine vein (Figs. 3b, d).

The sphenopalatine vein communicates near the mid-level of the paired nasopharyngeal ducts (Figs. 3a,b); at this level and rostrally the nasopharyngeal ducts have an exceedingly vascular lamina propria, containing enlarged venous sinuses (Figs. 3e, f). Rostrally, the nasopharyngeal ducts overlap a caudal portion of the maxilloturbinal. The paired nasopharyngeal ducts are more than half of the rostrocaudal length of the nasal fossa (Table 2).

## **Eptesicus fuscus (Vespertilionidae)**

In the histologically sectioned adult *Eptesicus*, the paired nasopharyngeal ducts begin at the level of the abrupt caudal end of the maxilloturbinal (Fig. 4a). The mucosa of the paired nasopharyngeal ducts contains numerous venous sinuses that surround all sides of the passageways (Fig. 4b). In addition, within a membranous septum dividing the ducts (Fig. 4c), a lymphatic mass occupies the lamina propria (Fig. 4d).

In the adult *Eptesicus* studied by diceCT, some parts of the nasopharyngeal airways are too indistinct to segment, particularly, in the pharynx. However, rostrocaudal end-points of the nasal fossa and paired nasopharyngeal ducts are evident and the paired ducts are less than half of the length of the nasal fossa (Table 2).

### **Phyllostomid bats**

Phyllostomids possess more abbreviated paired nasopharyngeal ducts than *Cynopterus* or *Eptesicus*. No portion of the maxilloturbinal resides within these paired ducts. Examination of the fetal *Desmodus* reveals that the sphenopalatine vein exits the nasal-nasopharyngeal airways rostral to the paired nasopharyngeal ducts (Fig. 5). Aligned histology and CT sectional/slice levels reveal that the sphenopalatine foramen traverses the palatine bone at about its mid-point in

rostrocaudal length (Figs. 5a, b, e). Rostral to this, the ventral part of the nasal fossa is highly vascular (Fig. 5d), whereas there are few sinuses found caudal to this level (Fig. 5f).

In all phyllostomids examined histologically, venous sinuses of the nasal mucosa are most numerous rostrally within the nasal fossa (Figs. 6a-d, h, i). They become more restricted ventrally nearer to the olfactory recess (Fig. 6e), and there are few sinuses present in the lamina propria of the paired nasopharyngeal ducts (Figs. 6f, g). One of the larger venous sinuses resides lateral to the vomeronasal organ. In *Glossophaga soricina* and *Monophyllus redmani* this sinus is especially large, in fact of larger cross-sectional area than the vomeronasal organ at some cross-sectional levels. Moreover, the venous sinus abuts the organ caudally where the vomeronasal cartilage is lacking (Figs. 6h, j). A three-dimensional reconstruction of *Anoura geoffroyi*, based on diceCT scans, reveals that this sinus is the septal collecting vein itself (Fig. 7).

The entirety of the nasal and nasopharyngeal passageways was reconstructed in 3D in four phyllostomids permitting a qualitative comparison. Compared to *Desmodus*, *Anoura* and *Leptonycteris* have narrower and more elongated airways (Fig. 8). *Desmodus* has greater dorsoventral height of the nasal cavity compared to the other phyllostomids. In contrast, both hipposiderids, *Triaenops* (Fig. 8) and *Hipposideros caffer* (not shown), have more rounded, dilated airways in all three regions assessed. The paired nasopharyngeal ducts are relatively restricted compared to the pteropodid *Cynopterus*.

Venous drainage pooled into lateral and septal collecting veins in all four species examined by three-dimensional reconstruction (Figs. 7, 8). In all bat species, the septal collecting veins receive a cascading series of septal sinuses that commence dorsally, and pass either rostroventrally (those that commence more caudally) or caudoventrally (those that commence rostrally) before ending in the septal collecting vein (Figs. 7a,c; 8). In sum, the array of sinuses has a fan-like distribution of drainage (Fig. 7c). The septal sinuses are particularly vast in distribution in *Anoura* and *Leptonycteris*. The lateral collecting vein receives venous sinuses of the maxilloturbinal, and drains caudally along the lateral side of the floor of the nasal fossa.

Although there are multiple small venous communications between the lateral and septal collecting ducts, most of the reconstructed species had a short, prominent communicating vein that drains the septal collecting vein into the lateral collecting vein (this communication could not be discerned in *Leptonycteris*). In *Desmodus* and the hipposiderid *Triaenops*, this communication occurs dorsally, as in the pteropodid *Cynopterus*. In *Anoura*, this communication occurs ventrally (Fig. 8). The lateral collecting vein then drains into the sphenopalatine vein near the caudal end of the nasal cavity (in all phyllostomids) or within the common nasopharyngeal duct (in all three hipposiderids, Figs. 8, 9). All three hipposiderid species had notably more venous networks within the nasopharyngeal ducts compared to phyllostomids.

# 3.2 Epithelial lining of nasopharyngeal region

In all bat species, the nasopharyngeal ducts are lined by respiratory epithelium (ciliated, pseudostratified, columnar) throughout their entire length (Figs. 10a-e). The degree of glandularity increases caudally in *Eptesicus* (Fig. 10c). In *Anoura* (Fig. 10f) and other phyllostomids, the respiratory mucosa of the nasopharyngeal ducts is lacking in vasculature compared to other bats, but *Anoura* possesses lymphatic masses (Fig. 10g).

Respiratory epithelium continues into the pharynx, but the portion of pharynx directly caudal to the oral cavity is lined with stratified squamous epithelium (Fig. 10h). In effect, bats have an extremely abbreviated nasopharynx and oropharynx.

## 3.3 Quantitative comparisons

Rostrocaudal lengths of the three airway segments reveal several trends in airway proportions. First, *Cynopterus* has the lowest disparity among segments among all bats; compared to other bat species, the paired nasopharyngeal ducts are notably longer (by 16% or more) in proportion to overall airway length (Fig. 11). Second, in *Triaenops* the common nasopharyngeal airway occupies by far the greatest proportion (40%) of total airway length, whereas in all other species its length varied between 16 and 24% of total airway length. Lastly, in all nasal emitting bats, there was a far greater disparity between nasal cavity length and paired nasopharyngeal duct length compared to *Cynopterus* (Fig. 11). Data on airway volumes in three species of bats support these findings (Fig. 11).

In this sample of bats, rostrocaudal nasal fossa and paired nasopharyngeal duct lengths increase as cranial length increases. The common nasopharyngeal airways depart from this trend notably (Fig. 12). However, a smaller subsample in which volumes could be obtained shows a dichotomy between volumes of the nasal cavity compared to paired nasopharyngeal ducts (Fig. 12).

#### 4 DISCUSSION

# 4.1 Can diceCT replace histology for identification of nasal epithelium or mucosa?

Progress in the study of nasal mucosal type distribution has been excruciatingly slow, despite many decades of efforts. Early works to quantify mucosa types were understandably focused on mammals of manageable size for histology, including various rodents, bats, shrews (e.g., soricids), and other small species (Adams, 1972; Bhatnagar and Kallen, 1975; Gross et al., 1982). Efforts to study larger species involved tissue sampling of individual structures, which allows rough characterization of individual turbinal function (e.g., Read, 1908; Negus, 1958; Loo, 1974; Kumar et al., 1993), but not the detailed overall quantification that serial sectioning allows. Only recently have larger mammals been studied at a similar level of detail. For example, Smith et al. (2011, 2014, 2019) quantified olfactory mucosa surface area in several species of

primates. Further, Van Valkenburgh and colleagues quantified olfactory surface area in a medium sized felid, a large canid, and the white-tailed deer (Van Valkenburgh et al., 2014; Pang et al., 2016; Yee et al., 2016). The recent broad quantitative analysis by Yee et al. (2016) demonstrated basic scaling patterns of olfactory surface area among mammals of diverse size, specifically that the percentage of olfactory surface area decreases with increasing body size. Even though this study used data from nearly five decades, it only included 27 data points collected using similar procedures. Obtaining more specific knowledge, for instance, concerning ecological correlates that may influence olfactory surface area (e.g., Eiting et al., 2014), appears daunting if it will require decades of additional histological study. Moreover, distortion can result from histological preparation, including differential shrinkage of individual internal structures (DeLeon and Smith, 2014). By extension, quantitative data derived from histology may be distorted to some extent.

The increased accessibility of diceCT methods has offered a new hope to more rapidly study soft tissue structures, while at the same time avoiding the permanently destructive nature of histological preparation (DeLeon and Smith, 2016; Hedrick et al., 2018). But, to date, the limits in resolution of tissue type using diceCT have been incompletely explored. It is demonstrable that diceCT does not allow identification of epithelium type, much less scrutiny of individual epithelial cells or the extent of cell layering (Yohe et al., 2019). However, if the epithelium plus the underlying lamina propria are considered together, the *mucosa* type can be inferred (e.g., based on the presence of compound, multicellular glands).

Here, we show that diceCT provides reliable information on vascular distribution in the mucosa of the nasal airways. Venous sinuses present dichotomously, depending on the presence of blood. The matching histological sections and diceCT slices of the fetal *Desmodus* demonstrate that blood as a tissue type is highly radiopaque following iodine uptake. Yet, blood is not always present within sinuses of preserved cadaveric material, as demonstrated in the adult *Cynopterus* (Fig. 2e, f). In matching diceCT slices, such vessels appear to have a dark lumen. By examining matching histology sections and diceCT slices, we also discerned that vessels that are less dense with blood may fade into gray levels of adjacent tissues in diceCT slices. This necessitated interpolation across slices to reconstruct the trajectory of sinuses. Three-dimensional reconstructions based on these indicators resulted in models that closely match venous sinus patterns observed in other mammals.

Thus, diceCT may, in the future, allow quantification of mucosa specialized for airwarming and for directing airflow. We would add that the availability of representative histological specimens of some species was greatly beneficial when interpreting structures in diceCT slices. We advocate the use of representative serially sectioned specimens to aid in interpretation in future studies, but it seems clear that diceCT can minimize the need to histologically section large samples, at least for the descriptive purposes employed here.

### 4.2 Venous distribution in nasal echolocating bats

In general, the venous drainage of the ventral airways had a common arrangement in all bats, suggesting it may be an ancestral condition. Since the organization in medial and lateral ventral drainage routes was previously described in the dog (Lung and Wang, 1989), this may be common and shared among mammals generally. The entire ventral airway is drained along large sinuses in the mucosa lining the septum and lateral wall. Rostrally, the lateral collecting vein receives a venous plexus associated with the maxilloturbinal, while the septal collecting vein receives a fan-shaped array of venous channels draining downward from the dorsal aspect of the septum.

While each of these routes is common to *Cynopterus* and the hipposiderid and phyllostomid species that we reconstructed, as well as the dog (Lung and Wang, 1989), there are some distinctions among species. First, there is a major difference in the nasal venous drainage of hipposiderids compared to all other bats examined. In both *Triaenops* and *Hipposideros*, the sphenopalatine vein receives the venous collecting veins at the level of the nasopharyngeal ducts. In addition, there are far more venous sinuses within the nasopharyngeal duct mucosa in the hipposiderids than in phyllostomids. This was visible in both species of *Hipposideros*, based on either histology or diceCT. The vast array of venous channels was seen in the paired and common portion of the nasopharyngeal ducts (pictured previously in the common portion by Curtis et al., 2020). The extent of the venous network in *Triaenops* was less apparent. However, smaller sinuses may have gone undetected in diceCT slices, and no histology was available. Nonetheless, the more caudal entry into the sphenopalatine vein suggests venous sinuses are functionally important in regions caudal to the nasal fossa in hipposiderids, unlike in phyllostomids.

A second distinction among species is seen in the septal network of veins. The septal plexus of veins has a similarly fan-shaped arrangement in all species. However, threedimensional reconstructions indicate it is more broadly distributed in Leptonycteris and Anoura than in *Desmodus*, reaching far more caudally in the former species which have an elongated skull. This could indicate a capacity to shift airflow unilaterally in these species if the sinuses are engorged on one side only. In most mammals, this is a mechanism known to prevent desiccation of nasal mucosa by alternating respiratory cycles of airflow (Eccles, 1996). The arrangement in Desmodus is more reminiscent of that in the dog (Lung and Wang, 1989) and is also more consistent with a distinct spatial separation of olfactory and respiratory regions seen in so-called "microsmatic" mammals (Craven et al., 2010). Another distinction, best seen in histology of two species (Anoura and Monophyllus), but readily apparent in diceCT scans of Anoura, is the relatively large septal collecting vein found adjacent to the vomeronasal organ. Previously, Bhatnagar and Smith (2007) noted the especially large size of this vein in cross-section, and placed it in the context of the lack of a cartilaginous or bony capsule for the vomeronasal organ at its caudal extent. In many mammals, this capsule places the vomeronasal organ within a semi-enclosed chamber in which pressure can be applied to its central lumen, thus creating the capacity to expel fluid or even pump nasal secretions (and odorants) inward (Salazar et al.,

2008). Bhatnagar and Smith (2007) suggested an enlarged venous sinus may be required in the absence of a surrounding capsule, to place pressure on the lumen from its lateral side. Here we document absence of the vomeronasal capsule at the caudal end of the vomeronasal organ in *Glossophaga* and *Monophyllus*, in combination with relative enlargement of the septal collecting duct. This provides more support for the hypothesis that enlargement of this sinus is functionally linked to vomeronasal organ. While this remains a qualitative observation, we have demonstrated it could be explored further using diceCT.

The venous network may also influence nasal airflow by providing for greater or lesser shrinkage of nasal mucosa in key regions of the nasal airway. For example, in humans the nasal valve area—which sits approximately 2 cm inside of the nostrils and controls airway access to the olfactory mucosa—is known to be heavily vascularized, particularly in the region of the nasal swell body, found near the junction between the nasal septal cartilage and the ethmoid (Saunders et al., 1995). This highly vascularized area may play an important role in governing access of respired air to key regions, such as the olfactory mucosa, though this question has been sparsely studied (Wexler and Davidson, 2004; Zhao and Frye, 2015). If differences in vascularization of key regions of the internal nose exist among bats, then they may similarly play outsized roles in governing access of airflow to various important parts of the nasal mucosa.

# 4.3 Division of labor within the nasal and nasopharyngeal airways

In some mammals, there are spatially distinct zones of airflow within the nasal fossa. These are thought to be influenced by turbinals, which have the dual capacity to direct airflow and to "interact" with air as it passes through the nasal fossa (e.g., condition air or detect odorants - Craven et al., 2007). Some mammals have distinctly separated olfactory and respiratory airstreams, at least during inspiration (Craven et al., 2010; Eiting et al., 2015). During inhalation, a more dorsal airstream delivers odorants to the ethmoturbinals, particularly the portions that are located within an *enclosed cul-de-sac* (the olfactory recess). This airstream is of relatively low velocity posteriorly, presumably to maximize odorant uptake (Craven et al., 2010; Eiting et al., 2015). A more ventral airstream is directed toward the nasopharynx. This air flows at a higher velocity, and is carried over the maxilloturbinals, which in most mammals is equipped with numerous venous sinuses that aid in conditioning air and thermoregulation in most mammals (e.g., Adams and Hochkins, 1983; Lung and Wang, 1989; Uraih and Maronport, 1990; Smith et al., 2007).

Not all mammals have such distinctly separated inspiratory airstreams (Pang et al., 2016; Smith et al., 2019). To some extent, this may relate to organization of the nasal fossa. In primates and felids, large portions of ethmoturbinals are found rostral to the olfactory recess (Pang et al., 2016; Smith et al., 2019). In contrast, the ethmoturbinals are mostly nested deep within the

olfactory recess in canids and rodents (Craven et al., 2007; Alvites et al., 2018), perhaps making it advantageous for conducting specific air streams.

In bats studied to date, relatively separate airstreams were found to exist during inhalation. However, during exhalation, unlike some extreme "macrosmats" such as canids and rodents, the expiratory airstreams were not so isolated, and in fact some expired air was predicted to interfere with inhaled air in some regions of the airway (Eiting et al., 2015). A relatively less investigated question is the extent to which the nasopharyngeal ducts and pharynx may assist the maxilloturbinal and adjacent respiratory mucosa-lined structures in conditioning inspired air.

The nasopharyngeal ducts, like the ventral meatuses directly rostral to them, are generally regions of high velocity airflow (Craven et al., 2010; Eiting et al., 2015). Here we document that in all bats, both these ducts and the pharynx are lined with respiratory epithelium, although the degree of vascularity of the lamina propria varies. Our findings do not support a hypothesis that all nasal echolocators generally have a highly vascular mucosa within the nasopharyngeal ducts. Instead, extensive vascularity is observed in the mucosa of these ducts in all except phyllostomid bats, which may be distinct in the relative dearth of venous sinuses with the nasopharyngeal ducts. Further work is needed to determine if phyllostomid bats are distinct from a broader array of bat taxa in this respect. If most bats have highly vascular nasopharyngeal passageways, it suggests the passageways are primitively associated with respiratory air-conditioning, rather than a nasal mode of echolocation.

In one sense, all echolocators have a greater spatial segregation of the nasal fossae and nasopharyngeal ducts. The nasopharyngeal ducts are devoid of any portion of turbinals in all echolocating bats examined here. Exceptions are known in *Rhinolophus*, which projects a freely extended turbinal segment deep into the nasopharyngeal duct (Curtis et al., 2020; also see Ito et al., 2021, who disagreed on the identity of this turbinal). In non-echolocating *Cynopterus*, the caudal maxilloturbinal is sequestered within the nasopharyngeal duct, as part of a highly vascularized region. The ventral nasal cavity airway and nasopharyngeal ducts are mutually interdependent since the latter, by definition, begins where a transverse lamina separates it from the olfactory recess. For this reason, it might be expected that they would have a collaborative functional role in mammals, at least in part. The reason that the nasal fossa and nasopharyngeal duct are more distinct in echolocating bats deserves more exploration.

In hipposiderids, there is a remarkable dilation of the caudal part (here termed the "common" part) of the nasopharyngeal duct, which continues at a similarly broad and volumetrically large space into the pharynx. We might expect that airflow throughout the entire nasal and nasopharyngeal airway to be slower in the two genera of hipposiderids studied here, although these taxa have yet to be studied via computational fluid dynamics. Another distinction of hipposiderids is the relatively truncated rostrocaudal dimensions of the nasal cavity. *Triaenops* scales well below the regression line for all the bats studied here, although volumetrically it may

differ less. This truncation and dilation of the nasal region and concomitant elongation of the nasopharyngeal ducts in Old World leaf-nosed and horseshoe bats (hipposiderids and rhinolophids) has been observed previously, and discussed in terms of sound transmission (Hartley and Suther, 1988; Pedersen, 1988). However, our findings suggest that the truncation of the rostral airspace may necessitate additional vascular mucosa caudally for conditioning of inspired air. This does not rule out more than only function for these sinuses. Based on their circumferential distribution, they could alter airway diameter, and could affect either airflow or possibly sound production.

Collaborative roles among nasal structures such as turbinals have frequently been discussed (Smith et al., 2007, 2019; Yee et al., 2016), and suggest species may "trade" respiratory function among different airway structures. The findings discussed here suggest the same may be true of different regions of the airway extending from the nasal cavity to the pharynx. The notion of shared functionality throughout the airspace deserves further exploration using larger samples of bats, in which the nasal airways of many species assume the additional function of echolocation. Our findings also show diceCT may offer a valuable tool for expanding the range of taxa to draw inferences on selection pressures that influence the morphology along this airspace.

#### REFERENCES

Adams, D.R., & Hotchkiss, D.K. (1983). *Journal of Veterinary Medicine*. C. Anatomia Histologia, and Embryologia, 12, 109-125.

Alvites, R.D., Caseiro, AR, Pedrosa, S.S., Branquinho, M.E., Varejao, A.S.P., & Mauricio, A.C. (2018). The nasal cavity of the rat and mouse-source of mesenchymal stem cells for treatment of peripheral nerve injury., 301:1678–1689.

Bhatnagar KP, & Kallen, FC. (1975). Quantitative observations on the nasal epithelia and olfactory innervation in bats. Acta Anat 91:272–282.

Bhatnagar, K.P., & Smith, T.D. 2007. Light microscopic and ultrastructural observations on the vomeronasal organ of *Anoura* (Chiroptera: Phyllostomidae). *Anatomical Record*, 290:1341-1354.

Bryant WS. 1916. The transition of the ciliated epithelium of the nose into the squamous epithelium of the pharynx. *Journal of Anatomy* 50: 172-176.

Cooper JG, Bhatnagar KP. 1976. Comparative anatomy of the vomeronasal organ complex in bats. *Journal of Anatomy* 122:571-601.

Craven BA, Neuberger T, Paterson EG, Webb AG, Josephson EM, Morrison EE, Settles GS. 2007. Reconstruction and morphometric analysis of the nasal airway of the dog (*Canis familiaris*) and implications regarding olfactory airflow. *Anatomical Record*, 290, 1325-1340.

Craven, B. A., Paterson, E. G. and Settles, G. S. (2010). The fluid dynamics of canine olfaction: unique nasal airflow patterns as an explanation of macrosmia. *J. Roy. Soc. Interface* 7, 933-943. Eccles R. 1996. A role for the nasal cycle in respiratory defense. *European Respiratory Journal*, 9, 371-376.

Eiting, T.P., Smith, T.D., & Dumont, E.R. (2014) Olfactory epithelium in the olfactory recess: a case study in new world leaf-nosed bats. *Anatomical Record* 297, 2105–2112.

Eiting, T.P., Perot, J.B., & Dumont, E.R. (2015). How much does nasal cavity morphology matter? Patterns and rates of olfactory airflow in phyllostomid bats. *Proceedings of the Royal Society B.* **282**2014216120142161

Gross, E.A., Swenberg, J.A., Fields, S., & Popp, J.A. (1982). Comparative aspects of the nasal cavity in rats and mice. *Journal of Anatomy* 135:83-88.

Hartley, D.J., & Suthers, R.A. (1988). The acoustics of the vocal tract in the horseshoe bat, Rhinolophus hildebranti. Journal of the Acoustical Society of America 84, 1201.

Hillenius, W.J. (1992). The evolution of nasal turbinates and mammalian endothermy. *Paleobiology* 18, 17–29.

- Ito, K., Tu, V.T., Eiting, T.P., Nojiri, T. & Koyabu, D. (2021). On the embryonic development of the nasal turbinals and their homology in bats. *Frontiers in Cell and Developmental Biology*, 9, 379, https://www.frontiersin.org/article/10.3389/fcell.2021.613545.
- Jurcisek, J.A., Durbin, J.E., Kusewitt, D.F., & Bakaletz L.O. (2003). Anatomy of the nasal cavity in the chinchilla. *Cells Tissues Organs*, 174, 136–152.
- Kumar, P., Kumar, S., & Singh, Y. (1993). Histological studies on the nasal ethmoturbinates of goats. *Small Ruminant Research*, 11, 85–92.
- Laitman, J.T., & Reidenberg, J.S. (1993). Specializations of the human upper respiratory and upper digestive systems as seen through comparative and developmental anatomy. *Dysphagia* 8, 318-325.
- Leela, K., & Kanagasuntheram, R. (1973). Some aspects of the histology of the nonhuman primate nasopharynx. *Acta Anatomica*, 84, 374-386.
- Leela, K., Kanagasuntheram, R., Khoo, F.Y. (1974). Morphology of the primate nasopharynx. *Journal of Anatomy*, 117, 333-340.
- Loo, S,K. (1974). Comparative study of the histology of the nasal fossa in four primates. *Folia Primatologica*, 21,290–303.
- Ma, X., & Li, T. (2106). The acoustical role of vocal tract in the horseshoe bat, Rhinolophus pusillus. *Journal of the Acoustical Society of America*, 139, 1264-1271
- Martinez, Q., Clavel, J., Esselstyn, J. A., Achmadi, A. S., Grohé, C., Pirot, N. & Fabre, P.-H. (2020). Convergent evolution of olfactory and thermoregulatory capacities in small amphibious mammals. *Proceedings of the National Academy of Sciences*, 1–8.
- Nakano, T. (1986). Ultrastructural studies of the transitional zone in the nasopharyngeal epithelium, with special reference to the keratinizing process in the mouse. *Acta Anatomica*, 127, 22-47.
- Negus, V. (1958). The comparative anatomy and physiology of the nose and paranasal sinuses. Edinburgh: Livingston.
- Pagano, A.S. (2014). The development and function of the nasopharynx and its role in the evolution of evolution of primate respiratory abilities. PhD. Dissertation, City University of New York.
- Pang, B., K. K. Yee, F. W. Lischka, N. E. Rawson, N.E., Kaskins, M.E., Wysocki, C.J., Craven, B.A., Van Valkenburgh, B. (2016). The influence of nasal airflow on respiratory and olfactory epithelial distribution in felids. *J Exp Biol* 219:1866-1874.
- Read, E.A. (1908). A contribution to the knowledge of the olfactory apparatus in dog, cat and man. *American Journal of Anatomy* 8, 17–47.

- Salazar, I., Sanchez-Quintero, P., Aleman, N., & Prieto D. 2008. Anatomical, immunohistochemical and physiological characteristics of the vomeronasal vessels in cows and their possible role in vomeronasal reception. *Journal of Anatomy*, 212, 686-696.
- Saunders MW, Jones NS, Kabala J, and Lowe J. 1995. An anatomical, histological and magnetic resonance imaging study of the nasal septum. Clin Otolaryngol 20:434–438.
- Smith, K.K. (1992). The evolution of the mammalian pharynx. *Zoological Journal of the Linnean Society*, 104, 313-349.
- Smith, T.D, Bhatnagar, K.P., Rossie, J.P., Docherty, B.A., Burrows, A.M., Mooney, M.P., Siegel, M.I. (2007). Scaling of the first ethmoturbinal in nocturnal strepsirrhines: olfactory and respiratory surfaces. *Anatomical Record* 290, 215-237.
- Smith, T.D., & Rossie, J.B. (2008). The nasal fossa of mouse and dwarf lemurs (Primates, Cheirogaleidae). *Anatomical Record* 291, 895-915.
- Smith, T. D., Eiting, T. P., & Rossie, J. B. (2011). Distribution of olfactory and nonolfactory surface area in the nasal fossa of *Microcebus murinus*: implications for microcomputed tomography and airflow studies. *Anatomical Record*, 294, 1217-1225.
- Smith, T.D., Eiting, T.P., & Bhatnagar, K.P. (2012). A quantitative study of olfactory, non-olfactory, and vomeronasal epithelia in the nasal fossa of the bat *Megaderma lyra*. *Journal of Mammalian Evololution*, 19, 27-41.
- Smith, T. D, Eiting, T. P. & Bhatnagar, K. P. 2015. Anatomy of the nasal passages in mammals. In *Handbook of Olfaction and Gustation*, 3<sup>rd</sup> Ed, ed. R. L. Doty, 37-62. New York: Wiley.
- Smith, T. D., B. A. Craven, S. M. Engel, and C. J. Bonar, & DeLeon, V.B. (2019). Nasal airflow in the pygmy slow loris (*Nycticebus pygmaeus*) based on a combined histological, computed tomographic and computational fluid dynamics methodology. *Journal of Experimental Biology*, 222. doi: 10.1242/jeb.207605.
- Smith, T. D., Curtis, A., Bhatnagar, K. P., & Santana, S. E. (2021). Fissures, folds and scrolls: the ontogenetic basis for complexity of the nasal cavity in a fruit bat (*Rousettus leschenaultii*). *Anatomical Record*, 304, 883-900.
- Van Valkenburgh, B., Pang, B., Bird, D., Curtis, C., Yee, K., Wysocki, C., & Craven, B. (2014). Respiratory and olfactory turbinals in feliform and caniform carnivorans: the influence of snout length. *Anatomical Record*, 297, 2065–2079.
- Vickerton, P., Jarvis, J., & Jeffery, N. (2013). Concentration-dependent specimen shrinkage in iodine-enhanced microCT. *Journal of Anatomy* 223:185–193.
- Wexler, D.B., & Davidson, T.M. (2004). The nasal valve: A review of the anatomy, imaging, and physiology. *American Journal of Rhinology*, 18, 143-150

Yohe, L.R., Hoffmann, S., & Curtis, A. (2018). Vomeronasal and olfactory structures in bats revealed by diceCT clarify genetic evidence of function. *Frontiers in Neuroanatomy*, 12, 32.

Yee, K.K., Craven, B.A., Wysocki, C.J., & Van Valkenburgh, B. (2016). Comparative morphology and histology of the nasal fossa in four mammals: gray squirrel, bobcat, coyote, and white-tailed deer. *Anatomical Record*, 299, 840–852.

Uraih, L.C., and Maronpot, R.R. (1990). Normal histology of the nasal cavity and application of special techniques. *Environmental Health Persepctives* 85, 187-208.

Zhao K, Frye RE. 2015. Nasal patency and the aerodynamics of nasal airflow in relation to olfactory function. In *Handbook of Olfaction and Gustation*, 3<sup>rd</sup> Ed, ed. R. L. Doty, 353-374. New York: Wiley.

# Figure legends

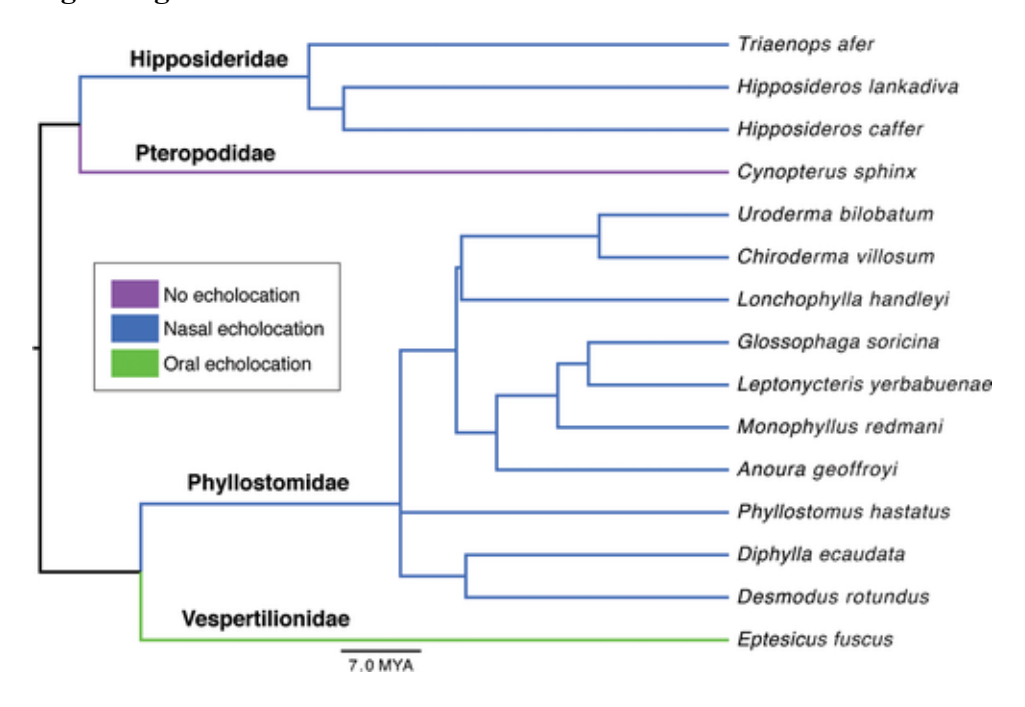


Figure 1: Cladogram of bat species and Families included in this study, with mode of echolocation. Tree topology from timetree.org.

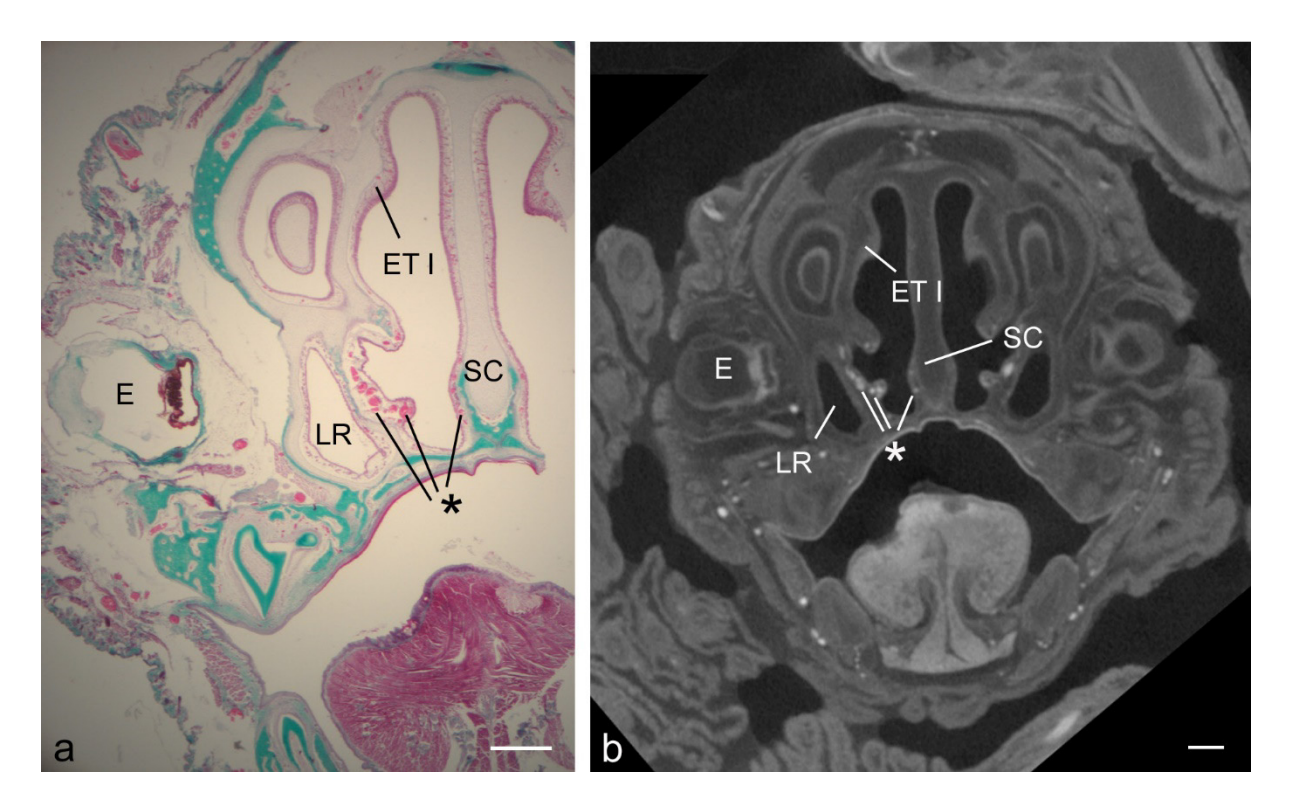


Figure 2: Histology sections (left) and diceCT sections (right) of a fetal *Desmodus rotundus* shown after diceCT is aligned to the same plane as histological sections. Note close match of landmarks such as the lateral recess (LR), the septal cartilage (SC), and the first ethmoturbinals (ET I) at its attachment to the roof of the nasal capsule. Also note venous sinuses (\*) are easily detected in the diceCT slice. E, eye. Scale bars: a, b, 1 mm.

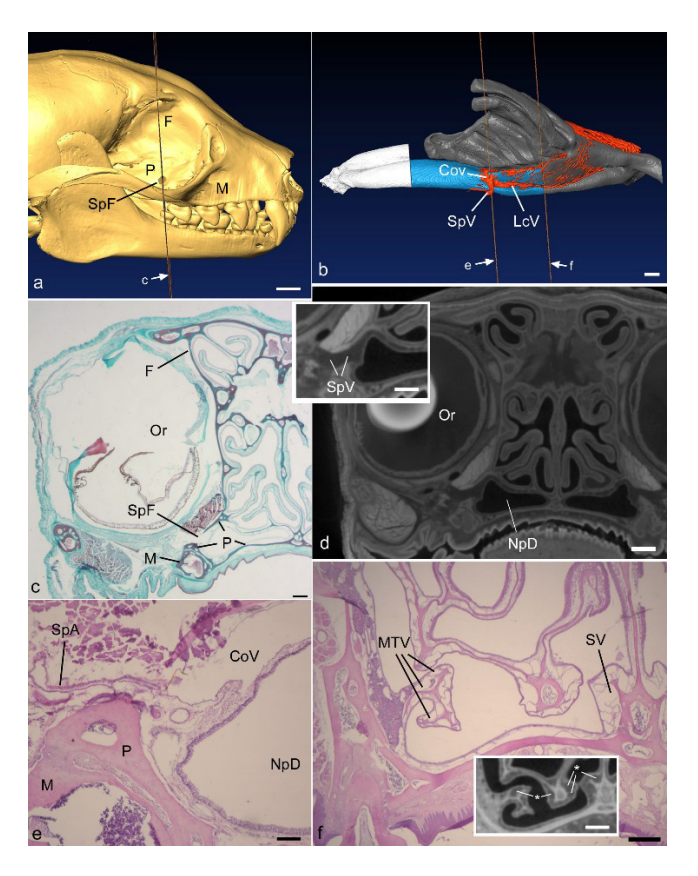


Figure 3: Skeletal anatomy and internal nasal anatomy of the face in adult Cynopterus sphynx. a) Lateral view of skull, with a line indicating a frontal plane through the sphenopalatine foramen (SpF). b) three-dimensional reconstruction of the nasal and pharyngeal passageways in the same specimen, with the airways encoded by gray (nasal cavity), paired nasopharyngeal ducts (blue; only the right side is shown) and common nasopharyngeal ducts/pharynx (white). Shown in a lateral view, the lateral collecting vein (LcV) is indicated near its terminus into the sphenopalatine vein (SpV). c, d) aligned histology and diceCT slices shown at the level of the plane shown in a. Inset for d: the sphenopalatine foramen (SpF) is indicated where it perforates the palatine bone (P). An enlarged view (insert) shows that the SpV is visible in the diceCT slice as a uniformly dark space. e) Magnified histological section just rostral to c, showing the sphenopalatine artery (SpA) and the venous sinuses within the nasopharyngeal duct (NpD). Note also the communicating vein (CoV) which connects the lateral collecting vein to the septal collecting vein (see plane indicated in b). f) Histological section just rostral to the NpD (see plane indicated in b). Inset for f: matching CT slice showing the lumina of venous sinuses appear as dark gray islands (\*). Note the numerous venous sinuses in the maxilloturbinal (MTV) which drain into the lateral collecting vein and septal venous sinuses (SV) which drain into the septal collecting vein. F, frontal bone; M, maxillary bone; Or, orbit; OR olfactory recess; S, nasal septum; TL, transverse lamina. Scale bars: a, 2 mm; b, 1 mm; c, 0.5 mm; d, 1 mm; e, 100 µm; f, 400 μm; insets, 0.5 mm.

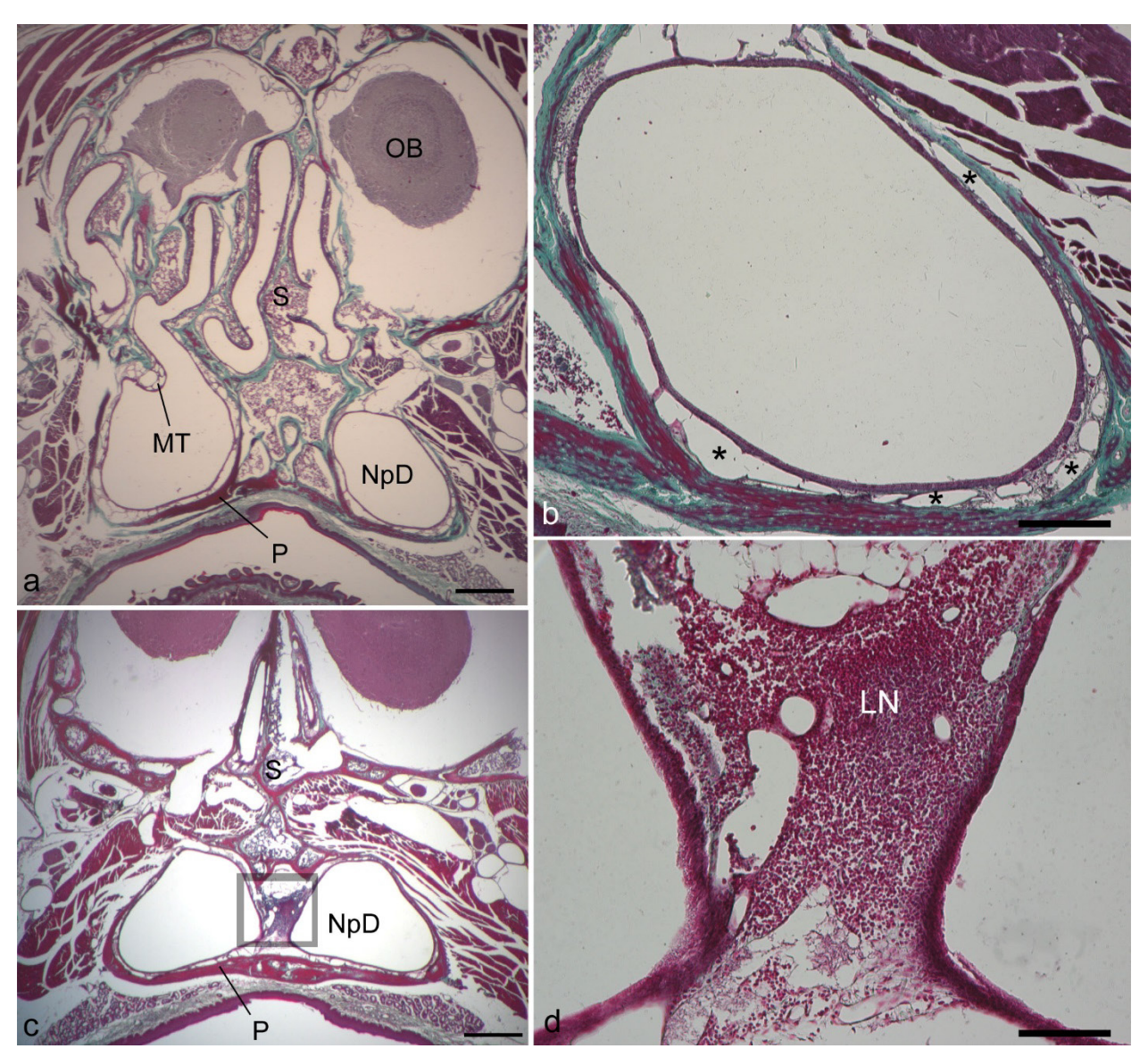


Figure 4: Micrographs of an adult *Eptesicus fuscus*, taken at the entrance to the paired nasopalatine ducts (**a**, **b**), and the ducts near the caudal end of the olfactory recess (**c**, **d**). **a**) The maxilloturbinal (MT) ends just rostral to the opening of the paired nasopharyngeal ducts (NpD). **b**) at this level, the NpD is surrounded on most sides by venous sinuses (\*). **c**) More caudally, the NpD still possess sinuses within the mucosa, but also in the mucosal septum that divides the paired ducts there is unencapsulated lymphatic tissue (**d**, enlarged form box in **c**). LN, lymphatic nodule; OB, olfactory bulb; P, palatine bone. Scale bars, a,c, 0.5 mm; b, 200 μm; d, 100 μm.

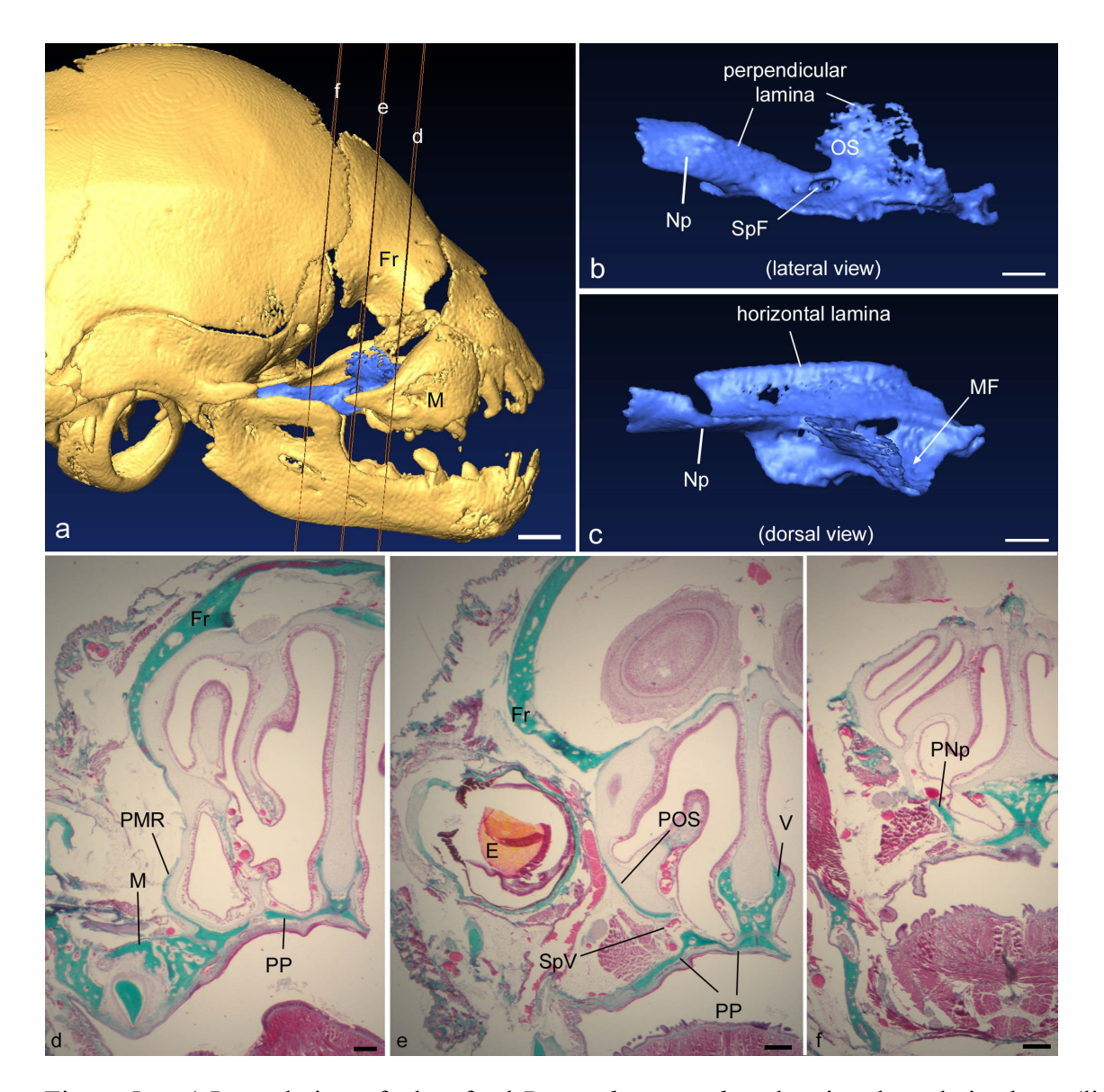


Figure 5: **a-c**) Lateral view of a late fetal *Desmodus rotundus*, showing the palatine bone (light blue) with three planes indicated, corresponding to histological sections shown in **d**, **e**, and **f** in the bottom row. The sphenopalatine foramen (SpF) is also indicated. **b**) The palatine bone, isolated, in lateral view. The perpendicular lamina is emphasized, with a caudal part that borders the nasopharyngeal duct (Np). **c**) In a dorsal view, the horizontal lamina is emphasized. Rostrally, the perpendicular lamina is a fan-shaped plate, with an orbital surface (OS) facing laterally. Most rostrally, this plate has a concavity on the medial surface, the maxillary fossa (MF). The horizontal lamina forms much of the hard palate (**c**). **d**) In the most rostral slice level indicated in plate **a**, the palatine supports the maxillary recess (PMR) and forms part of the palate (PP). **e**) In the middle slice, the orbit is transected (E, eye), and the palatine forms the ventromedial orbital wall (POS), and still contributes to the palate (PP). **f**) Most caudally, the horizontal lamina (and the palate) ends, but the perpendicular lamina (PNp) continues and supports the nasopharyngeal ducts. Scale bars: a, a, 1 mm; b, 3, 0.5 mm; d-f, 300 μm.

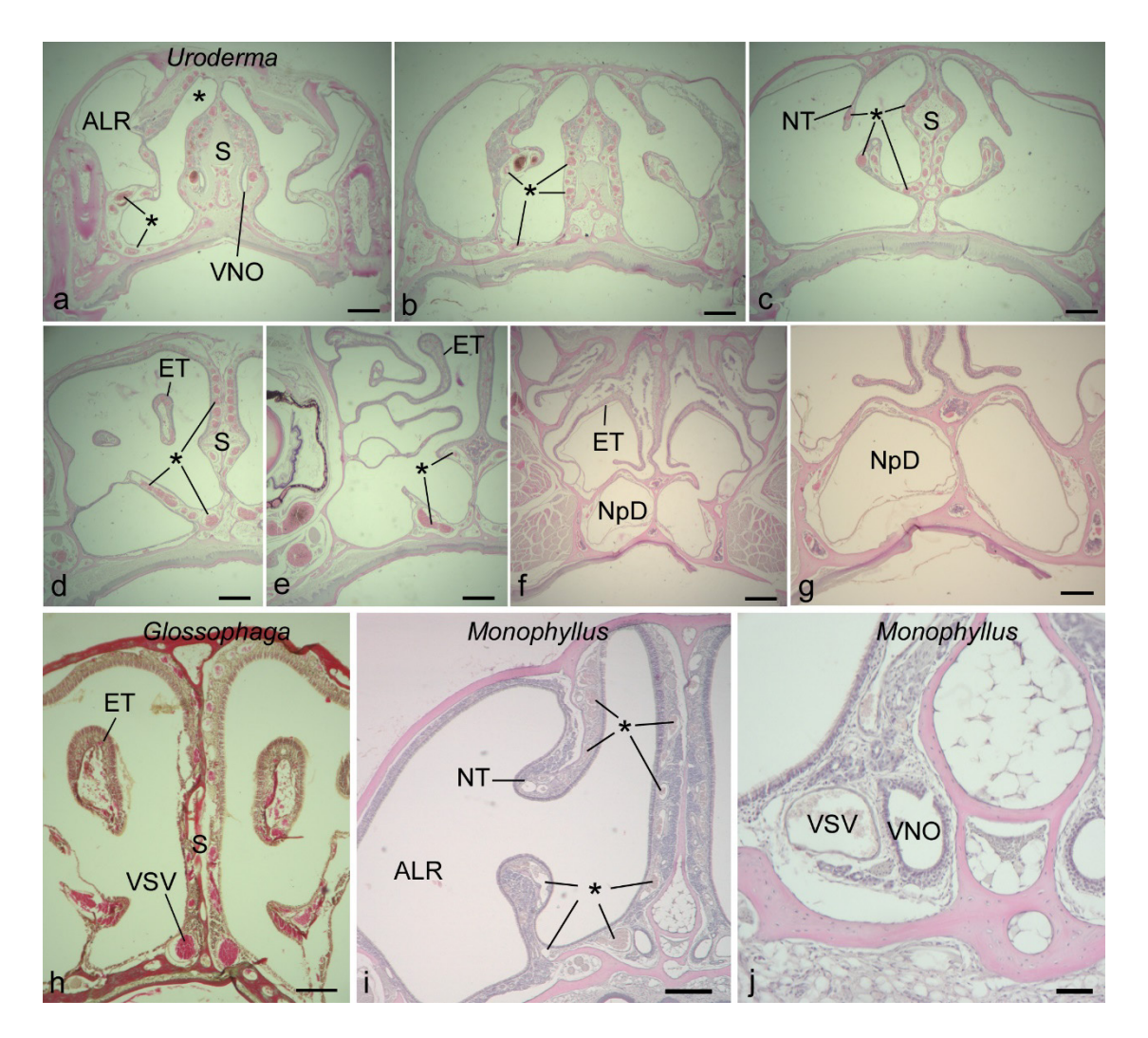


Fig. 6: Distribution of venous sinuses in various phyllostomids. **a-g**) *Uroderma* is shown as a rostrocaudal series of histological sections. Rostrally (**a, b**), venous sinuses (\*) are distributed from the floor to the roof of the nasal fossa, but not within the anterolateral recess (ALR). Caudal to this recess, the nasal fossa is broad (**c**) but sines are restricted close to the midline, along the nasal septum (S), the nasoturbinal (NT) and within the mucosa of alar processes that project from the base of the septum. In the rostral part of the ethmoturbinal (ET) region (**e-f**), sinuses become progressively restricted ventrally. At the level of the olfactory recess (**g**), few sinuses are observed. **h**) Rostral nasal fossa in *Glossophaga*, showing a broad dorsoventral distribution of venous sinuses, and the sinus of the vomeronasal organ (VSV = enlarged septal collecting duct). **i**, **j**) Rostral nasal fossa of *Monophyllus*, showing venous sinuses restricting to the nasal fossa, and lacking in the ALR, and the VSV adjacent to the vomeronasal organ. Scale bars: a-h, 5mm; I, 250 μm; **j**, 50 μm.

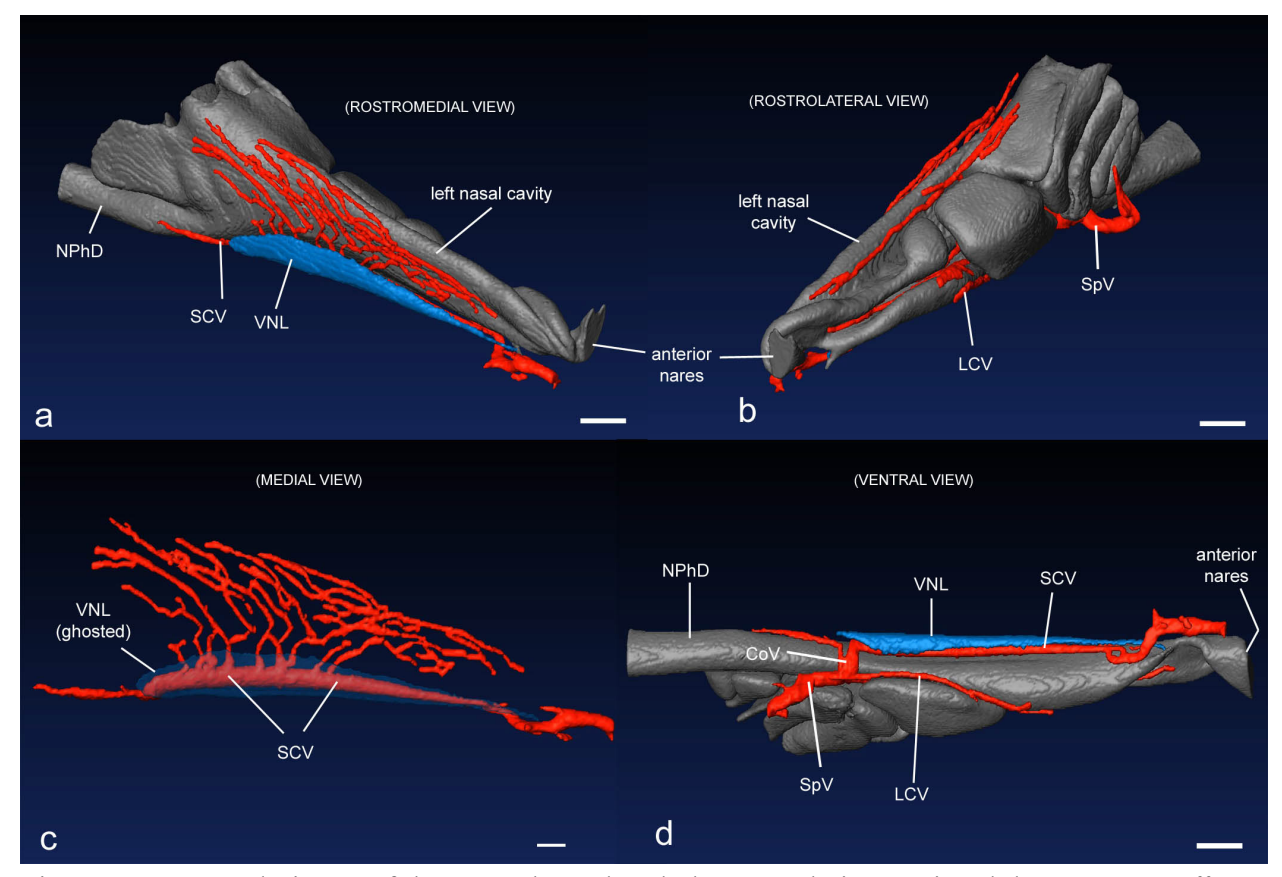


Figure 7: Venous drainage of the ventral nasal and pharyngeal airways in adult *Anoura geoffroyi*, reconstructed from a diceCT scan. Top: rostromedial (a) and rostrolateral (b) views showing the septal collecting veins (SCV), which drains the septal venous plexus and the lateral collecting vein (LCV) which receives drainage form the maxilloturbinal. Both collecting veins drain into the sphenopalatine vein (SpV). The SCV is intimately associated with the vomeronasal organ (blue = lumen of left vomeronasal organ, VNL). c) the VNL is ghosted to show the SCV, which is immediately lateral to it, receiving venous sinus drainage from the septal mucosa. d) a short communicating vein (CoV) connects the lateral and septal collecting veins to the sphenopalatine vein. Scale bars: a, b, d, 1 mm; c, 0.5 mm.

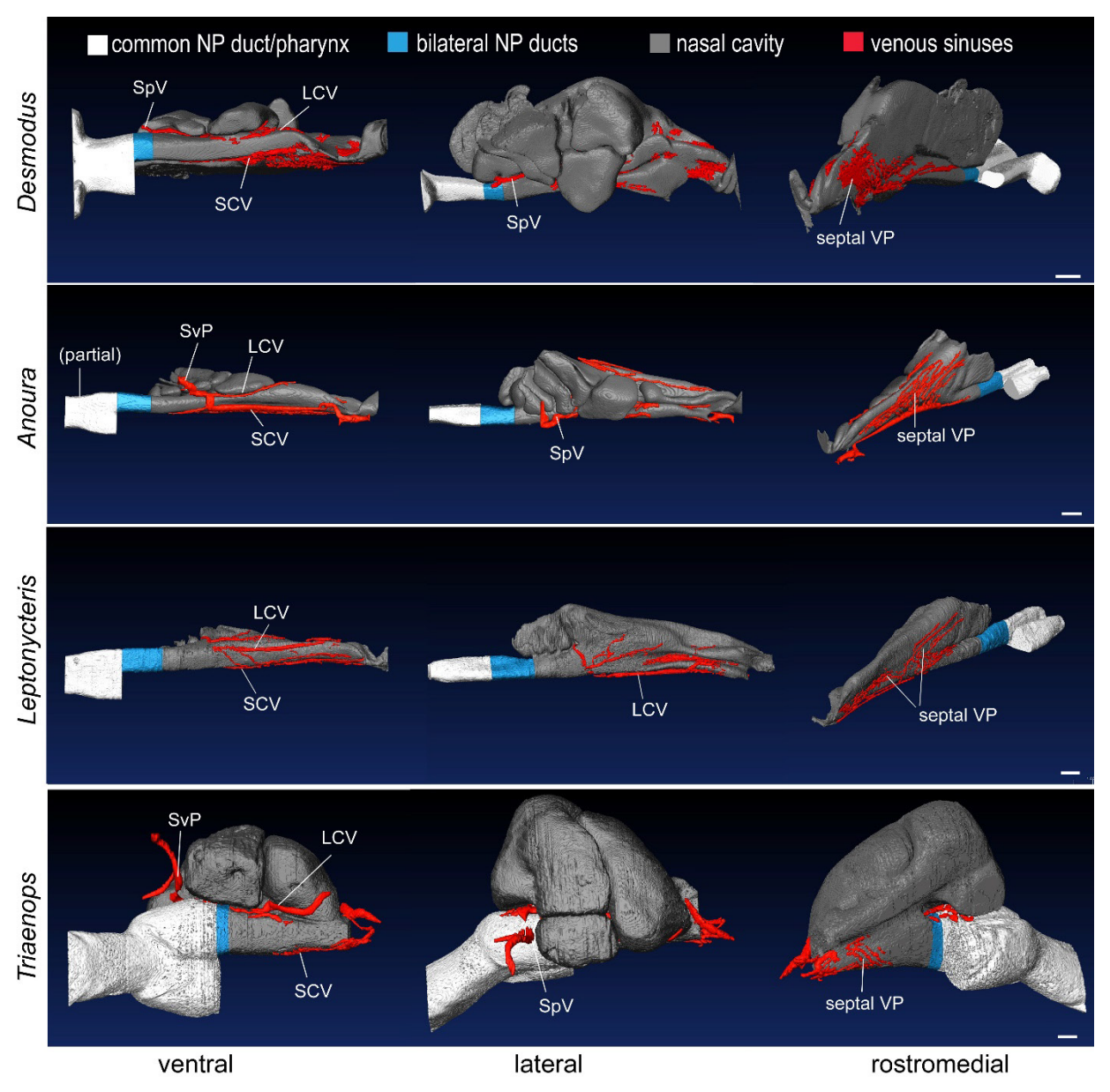


Figure 8: Color-coded reconstructions of the nasal and pharyngeal airways in four adult bats, also showing venous drainage of the ventral airways. Nasal airways are nearly telescoped in *Anoura geoffroyi*, and extremely dilated in *Triaenops afer*. The septal venous plexus (SpV) drains obliquely down and rostrally, into the septal collecting vein (SCV). The SCV veers laterally to unite with the lateral collecting vein (LCV) to form the sphenopalatine vein (SpV). Scale bars: top three rows, 1 mm; bottom row, 0.5 mm.

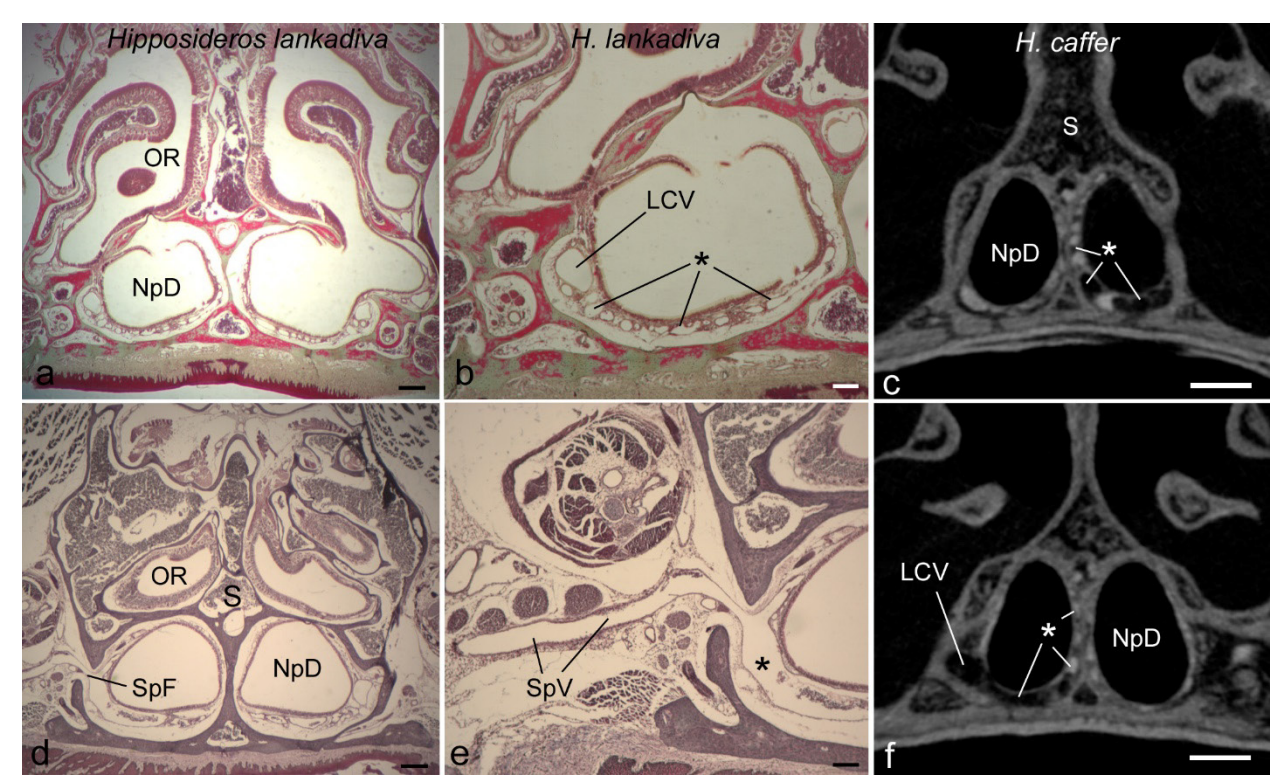


Fig. 9: Paired nasopharyngeal ducts (NpD) in *Hipposideros lankadiva* (**a, b, d, e**) and *H. caffer* (**c, f**). Both histology (**a, b, d, e**) and diceCT slices reveal venous sinuses (\*) in the mucosa on all sides of the NpD. The sphenopalatine foramen (SpF, **d**) communicates with the ducts, as in *Cynopterus*. LCV, lateral collecting vein; OR, olfactory recess; S, nasal septum; SpV, sphenopalatine vein. Scale bars: a, d, 300 μm; b, e 150 μm; c, f, 0.5 mm.

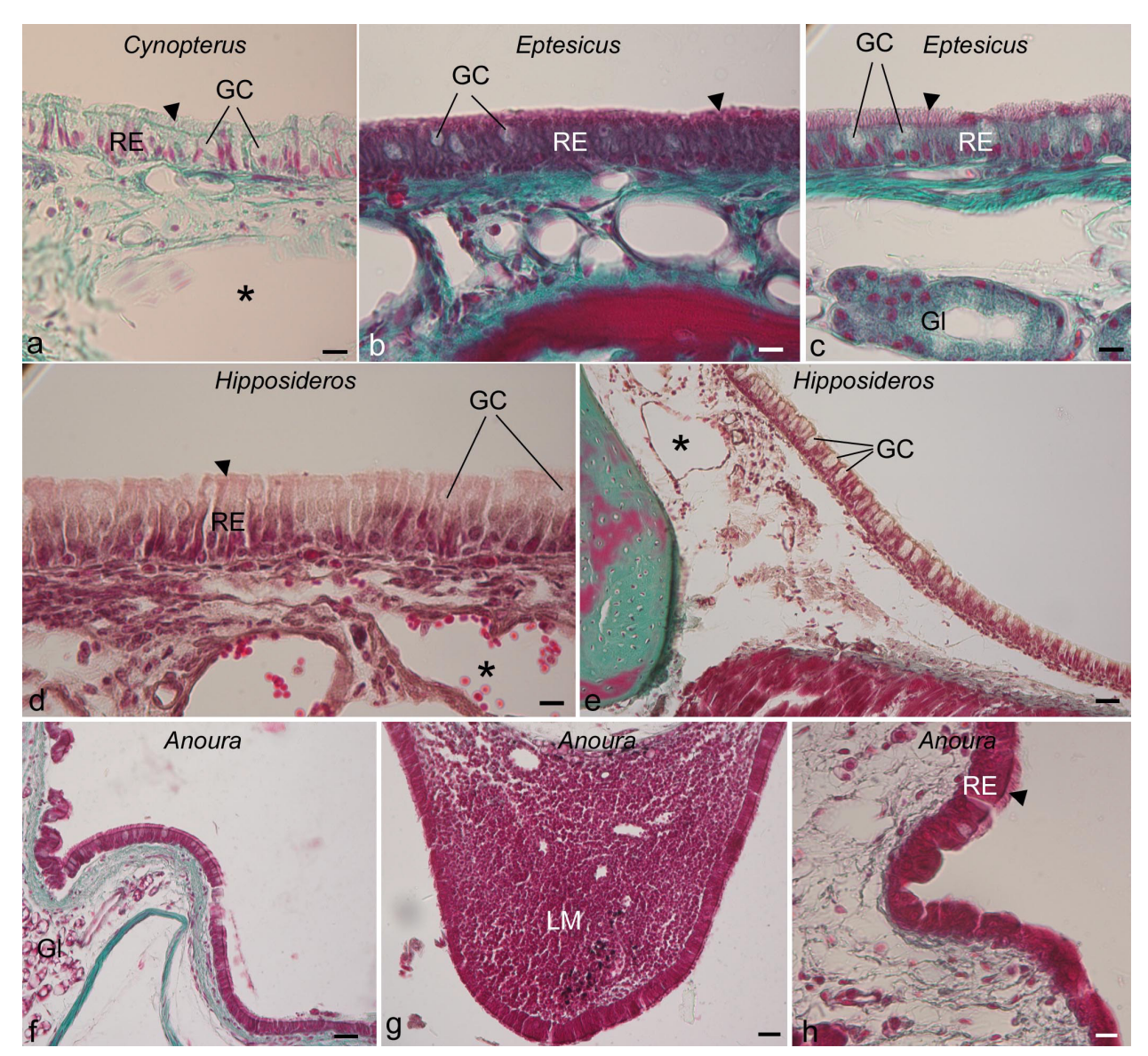
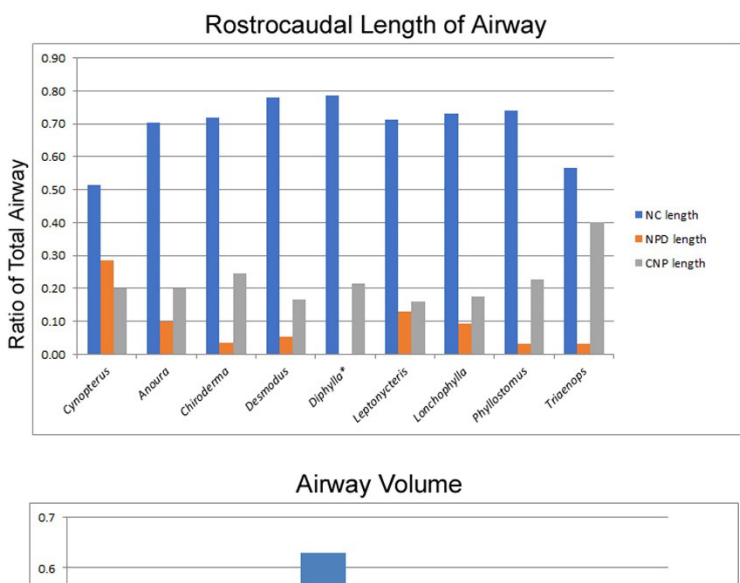


Figure 10: High magnification views of the epithelium of the nasopharyngeal passages (= nasopharyngeal ducts and pharynx) in bats. High magnification views of the nasopharyngeal ducts of a) *Cynopterus*, b, c) *Eptesicus*, d) *Hipposideros*, showing respiratory epithelium (RE; arrowhead = cilia). Note underlying venous sinuses; *Eptesicus* becomes increasingly glandular caudally. e) More caudal section of the nasopharyngeal duct in *Hipposideros*, still showing respiratory epithelium (GC = goblet cells). f, g) Nasopharyngeal duct of *Anoura*: f) with respiratory mucosa lacking in sinuses; g) partial mucosal septum in common nasopharyngeal duct, including lymphatic masses (LM) with the lamina propria. h) Pharynx in *Anoura* where it communicates with region caudal to oral cavity; note transition to non-ciliated epithelium. Scale bars: a-d, h,  $10 \mu m$ ; e, f, g,  $30 \mu m$ .



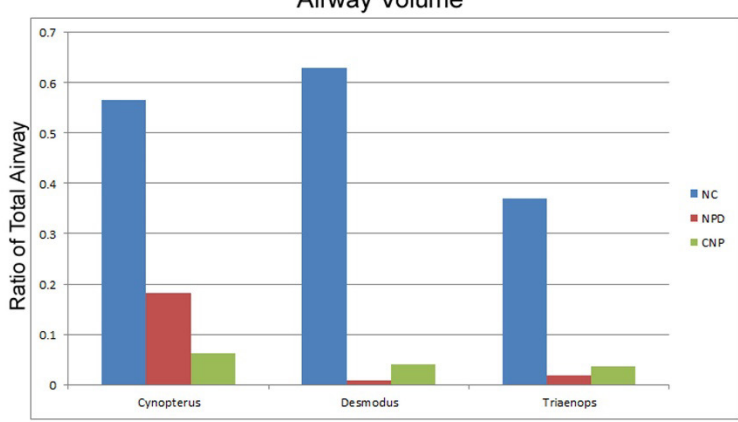


Figure 11: Proportions of the nasal and nasopharyngeal airways in bats. At top, ratios of rostrocaudal length of airway segments. At bottom, volumes of the three airway segments (including entire olfactory recess) expressed as a ratio of total airway volume. Measurements are from one side of the nasal cavity only; NC, nasal cavity; NPD, paired nasopharyngeal duct; CNP, common nasopharyngeal duct and pharynx (volume = x 0.5). \*, *Dyphylla* lacked a paired nasopharyngeal duct.

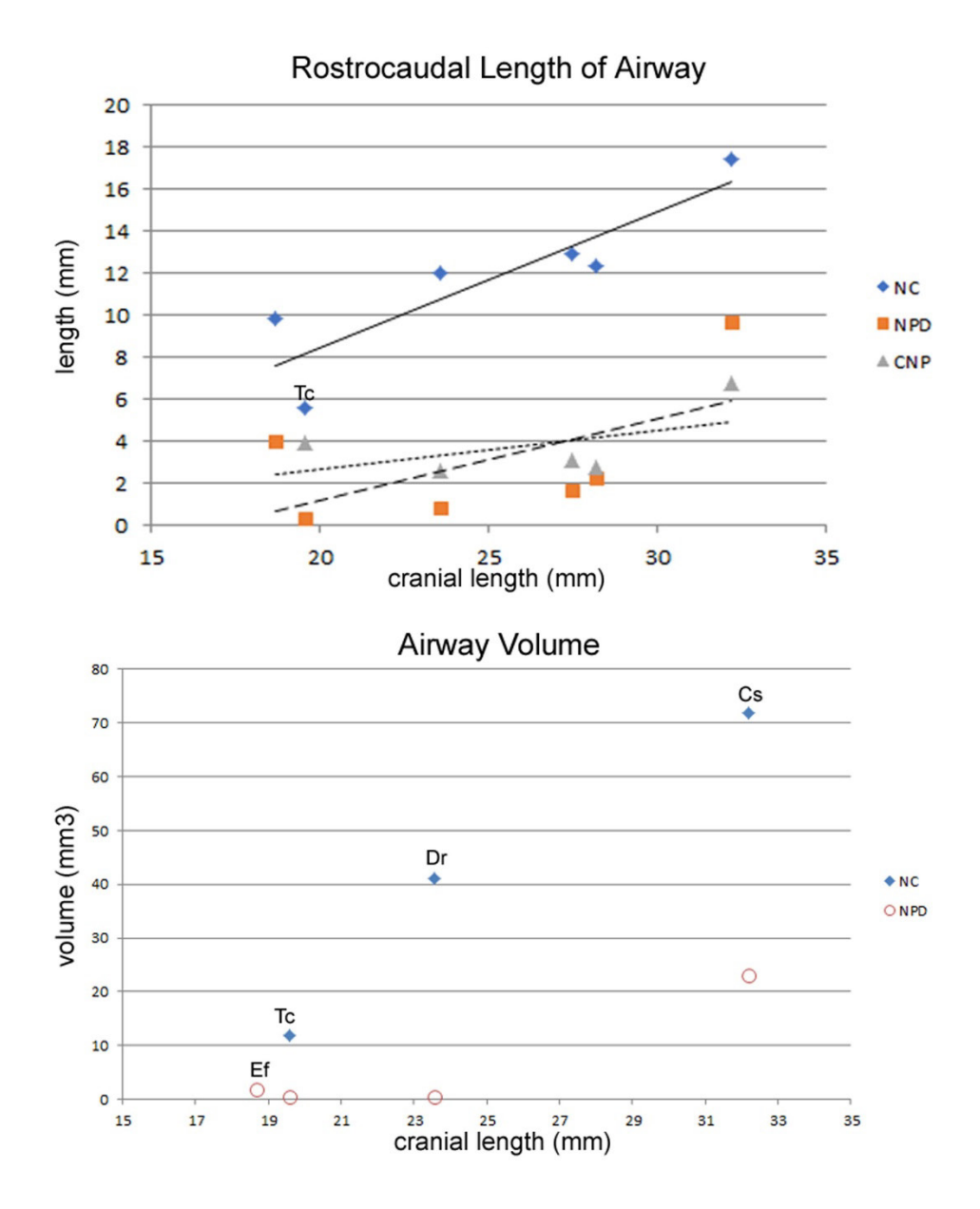


Figure 12: Plots of airways segment rostrocaudal length (top) and volume (bottom) against cranial length. Measurements are from one side of the nasal cavity only; NC, nasal cavity; NPD, paired nasopharyngeal duct; CNP, common nasopharyngeal duct and pharynx (volume = x 0.5). Cs, *Cynopterus sphinx*; Dr, *Desmodus rotundus*; Ef, *Eptesicus fuscus*; Tc, *Triaenops caffer*. Lines for linear regression equations for each airway segment are indicated: solid line = nasal cavity; long dashed line = NPD; short dashed line = CNP.